University of Pennsylvania, Philadelphia, PA, USA.
In order to assess how lever arm length affects the three-dimensional motions of myosin V during processive motility, two constructs were studied using single molecule polarized total internal reflection fluorescence (polTIRF) microscopy. MyoV6IQ and MyoV4IQ contain 6 and 4 calmodulin (CaM) binding IQ motifs, and otherwise consist of the native myosin V excluding the tail domain. Bifunctional rhodamine labeled CaM replaced a native CaM, giving probe angles β_P relative to the actin axis and α_P, the azimuth around actin. As with other processive myosins, α_P and β_P exhibited tilting of the probe with each step. With MyoV6IQ, α_P often returned to its initial value after two steps, as expected for nearly straight walking. This behavior enabled us to determine the orientation of the lever arm, α_L and β_L, as well as θ_L and f_L, the probe angles relative to CaM. β_L was 100° and 40° in the leading and trailing heads, respectively. In MyoV4IQ, β_P was similar to 6IQ, but α_P seldom returned to its earlier value after two steps. This indicates considerable net azimuthal rotation, as expected for smaller step sizes. Thus, lever arm length determines the azimuthal angular path, whereas the axial orientation is likely determined by structural constraints in the motor domain. Modified gliding filament assays were performed using polTIRF to detect twirling of actin about its axis during motility. MyoV6IQ twirled almost exclusively left-handed with a pitch of 1.4 μm. MyoV4IQ twirled with both right- and left-handed pitches of 1.0 and 1.2 μm, respectively. Bidirectional twirling of MyoV4IQ contrasts with every isoform of myosin previously tested (II, native V, VI and X) all of which twirled with a single handedness. This work was supported by NIH grant AR05117.

732-Pos Board B611
Structural and Mechanistic Determinants of Myosin VI Processivity and Anchoring
Peiying Chuan, Alexander R. Dunn, Zev Bryant, James A. Spudich.
Stanford University School of Medicine, Stanford, CA, USA.
Myosin VI is a molecular motor that can function both as a transporter and anchor in cells. Its role is regulated through load, being capable of taking multiple consecutive 36 nm steps along an actin filament under zero load and switching to an anchor by stalling when placed under piconewton levels of load. The parameters necessary for such processivity and anchoring are not fully understood. We use high-speed gold nanoparticle tracking to study single molecules of myosin VI with millisecond resolution in the absence of load. Optical tweezers are used to observe the behavior of the molecules when perturbed by load. In order to probe the contribution of the myosin VI tail domain to processivity and anchoring, we have created and characterized a number of mutant tail domain constructs. Our results reveal the resiliency of myosin VI as a transporter and suggest that it has evolved its unusual tail domain for purposes other than efficient cargo transport in the absence of applied load. We present preliminary data investigating the role of the myosin VI tail domain in important cellular processes such as transport against load and load-induced anchoring.

733-Pos Board B612
Myosin VI Dimerizes And Walks Processively Along Actin
Monalisa Mukherjea[1], Daniel Safer[1], Julie Ménétrey[2], Paola Llinas[2], Anne Houdusse[2], H. Lee Sweeney[1].
[1]Univ. of Pennsylvania, Philadelphia, PA, USA, [2]Structural Motility, Institut Curie CNRS, Paris, France.
Myosin VI is an unconventional motor protein that can move processively along the actin filament in an opposite direction towards the minus-end, contrary to all other known myosins. Despite its short lever arm, represented by a single IQ domain, myosin VI demonstrates large step sizes (30-36nm), typically characteristic of motor proteins with longer lever arms, viz. myosin V with 6 IQ domains. In cells, myosin VI is involved in diverse functions including Golgi transport, endocytosis and stereocilia maintenance. Though it is possible that myosin VI can function either as a dimer or a monomer in cells, based on our studies on the functional properties of the protein, it is likely that a dimeric protein can undergo intramolecular strain to become a more efficient actin anchor which makes it more competent as a transporter. Previous studies from our lab have shown that both full-length as well HMM fragments are capable of forming stable, processive dimers upon clustering, indicating that myosin VI monomers need to be in close proximity to initiate dimerization. Our recent studies show dimerization of full-length myosin VI can be triggered by cargo binding and the cargo-bound motors walk processively on actin filaments with the expected step size. Following the IQ motif, the lever arm extension of about hundred amino acid residues contains the sequence sufficient for dimerization. However, the accurate location of dimer formation remains controversial since the putative dimerization domain in myosin VI has non-native coiled-coil sequences. Our working hypothesis is that dimerization triggers the unfolding of a 3-helix bundle creating the 12nm extension required for proper myosin VI walking. Based on a series of truncations, we are in the process of testing this hypothesis and defining the nature and sequence of the dimerization domain.

734-Pos Board B613
Cryo-Electron Microscopy of Myosin 5 on Actin
Kavitha Thirumurugan[1], Stan A. Burgess[1], Fang Zhang[2], James R. Sellers[2], **Peter J. Knight**[1].
[1]Astbury Centre, University of Leeds, Leeds, United Kingdom, [2]Lab of Molecular Physiology, NHLBI, NIH, Bethesda, MD, USA.
Single molecules of myosin 5 move processively along actin filaments by a hand-over-hand mechanism. In an earlier study we found by negative staining that at micromolar, rate limiting ATP concentrations both heads of the HMM fragment of myosin 5 were attached to actin, usually 13 actin subunits apart and the leading head had its converter subdomain in a pre-powerstroke position with variable leading lever conformation. To determine whether any of these results were artefacts of our experimental method, we have now gathered data by cryo-EM of unstained samples flash frozen at saturating (0.2 mM) ATP concentrations and low calcium concentrations. We used full length mouse myosin 5a (melanocyte isoform), expressed in sf9 cells. From our recent work, we expect many molecules to be detached from actin and folded into a triangular shape, and some molecules to be unfolded and actively moving along actin. We observe both forms of molecule. Unfolded molecules attached to actin by both heads were analyzed by single particle methods. The heads are mostly spaced 13 actin subunits apart with small proportions at 11 and 15 subunit spacings. Trailing heads, expected to contain ADP under these conditions in contrast to no nucleotide in our earlier study, have the conformation expected for post-powerstroke heads, and straight levers. Levers of leading heads emerge from the motor domain at a pre-powerstroke position and are somewhat curved. The initial segment of the tail is sometimes visible. It is usually angled in the trailing direction, as noted in negative stain, suggesting that the head-tail junction of active molecules is not a freely mobile joint. These results confirm and refine our earlier conclusions. Supported by the Wellcome Trust (076057).

Ion Motive ATPases

735-Pos Board B614
Kinetic Analysis Of ATP Synthesis Catalyzed By E. coli FoF1 ATP Synthase Reconstituted Into Egg Yolk Liposomes: Evidence For Bi-site Activation
Mikhail Galkin, Robert K. Nakamoto.
University of Virginia, Charlottesville, VA, USA.
Escherichia coli F_OF_1 ATP synthase was reconstituted into liposomes made of asolectin, soybean PC or egg yolk PC. The reconstitution system with egg yolk proteoliposomes gave the highest ATP synthase activity and ATP yield, and was used for analysis of the reaction characteristics. Under optimal conditions (ΔpH 3.4 at 37°C, $\Delta\Psi = 109$ mV, 10 μM valinomycin), the steady state rate of ATP synthesis reached 400 s^{-1}. The dependency for Pi was hyperbolic over a range from 0.01 -5 mM. In contrast, variation of ADP concentration over a broad range (20 nM-2000 μM) revealed two apparent K_m, one much less than 1 μM and the second at 11 μM. The apparent K_m values for both substrates were independent of the membrane potential, $\Delta\Psi$. We propose that filling of two catalytic sites is sufficient and necessary for steady state ATP synthesis. Also, thiophosphate was found to be an uncompetitive inhibitor of ATP synthesis with respect to ADP, which implies an ordered substrate binding with ADP binding preceding phosphate binding. The data are in agreement with a reversible ATP synthesis-hydrolysis catalytic step with the ratio of the forward and reverse rate constants close to unity (Baylis Scanlon et al. *J. Biol. Chem.* 283, 26228-26240, 2008). In contrast to ATP hydrolysis where binding of Mg·ATP to the third catalytic site drives rotational catalysis, our results show that steady state ATP synthesis only requires binding of substrates to the second site.

736-Pos Board B615
Ca^{2+} Binding to Site I of the Cardiac Ca^{2+} Pump (SERCA2a) is Sufficient to Dissociate Phospholamban (PLB)
Zhenhui Chen, Brandy L. Akin, Larry R. Jones.
Indiana University, Indianapolis, IN, USA.
Our model of mutually exclusive binding of PLB and Ca^{2+} to SERCA2a suggests that the Ca^{2+}-bound form of SERCA2a (E1) cannot interact with PLB. However, it is unclear whether Ca^{2+} binding to site I, site II, or both sites of SERCA2a is sufficient to dissociate PLB. To investigate this, we made several SERCA2a mutants: mutants lacking Ca^{2+} binding site I (E770Q or T798A), Ca^{2+} binding site II (E309Q or N795A), or both sites (D799N, or E309Q, E770Q double mutant). When individually expressed in insect cell microsomes, all these mutants failed to transport Ca^{2+}, but were readily phosphorylated by Pi to form E2~P (measured in Ca^{2+}-free buffer favoring formation of E2, the low Ca^{2+} affinity conformation). Ca^{2+} inhibition of E2~P formation

was maintained with all site II mutants, but was lost with site I mutants, demonstrating that Ca^{2+} binding to site I is sufficient to prevent E2~P formation. On the other hand, N30C-PLB cross-linked strongly to all Ca^{2+} binding site mutants, including those lacking either site I, site II, or both sites, thus demonstrating that PLB binds preferentially to E2, the Ca^{2+}-free state of SERCA2a. 10 μM Ca^{2+} blocked cross-linking of N30C-PLB to site II mutants, yielding K_{Ca} values of 1.25 ± 0.3 μM for E309Q, and 0.32 ± 0.03 μM for N795A, compared to 0.44 ± 0.04 μM for WT-SERCA2a. However, Ca^{2+} had no effect on cross-linking of N30C-PLB to SERCA2a with site I mutants, even at Ca^{2+} concentrations of 100 μM or higher. These results demonstrate that Ca^{2+} binding site I of SERCA2a is the key Ca^{2+}-binding site regulating PLB association and dissociation.

737-Pos Board B616

Concerted but Noncooperative Activation of Nucleotide and Actuator Domains of the Ca-ATPase Upon Calcium Binding

Baowei Chen[1], James E. Mahaney[2], M. Uljana Mayer[1], Diana J. Bigelow[1], **Thomas C. Squier[1]**.
[1]Pacific Northwest National Laboratory, Richland, WA, USA, [2]Virginia College of Osteopathic Medicine, Blacksburg, VA, USA.

Calcium-dependent domain movements of the actuator (A) and nucleotide (N) domains of the SERCA2a isoform of the Ca-ATPase were assessed using constructs containing engineered tetracysteine binding motifs, which were expressed in insect High-Five cells and subsequently labeled with the biarsenical fluorophore 4′,5′-bis(1,3,2-dithoarsolan-2-yl)fluorescein (FlAsH-EDT_2). Maximum catalytic function is retained in microsomes isolated from High-Five cells and labeled with FlAsH-EDT_2. Distance measurements using the nucleotide analog TNP-ATP, which acts as a fluorescence resonance energy transfer (FRET) acceptor from FlAsH, identify a 2.4 Å increase in the spatial separation between the N- and A-domains induced by high-affinity calcium binding; this structural change is comparable to that observed in crystal structures. No significant distance changes occur across the N-domain between FlAsH and TNP-ATP, indicating that calcium activation induces rigid body domain movements rather than intradomain conformational changes. Calcium-dependent decreases in the fluorescence of FlAsH bound respectively to either the N- or A-domains indicate coordinated and noncooperative domain movements, where both A- and N-domains display virtually identical calcium dependencies (i.e., $K_d = 4.8 \pm 0.4$ μM). We suggest that occupancy of a single high-affinity calcium binding site induces the rearrangement of the A- and N-domains of the Ca-ATPase to form an intermediate state, which facilitates phosphoenzyme formation from ATP upon occupancy of the second high-affinity calcium site.

738-Pos Board B617

FRET from SERCA to Phospholamban is Decreased by Thapsigargin and Anti-PLB Antibody, but not by Calcium

Philip Bidwell, Daniel J. Blackwell, Zhanjia Hou, Seth L. Robia.
Loyola University Chicago, Maywood, IL, USA.

To investigate the regulation of SERCA by phospholamban (PLB) we measured FRET from CFP-SERCA to YFP-PLB. In permeabilized cells, anti-PLB antibody significantly decreased SERCA-PLB FRET consistent with other groups' chemical crosslinking, immunoprecipitation (IP), and functional assays. However, FRET was not abolished by millimolar calcium, suggesting that PLB still interacts with calcium-bound pump. This result contrasts with crosslinking and IP results, but is in harmony with another lab's in vitro FRET studies. In intact cells, SERCA-PLB FRET was decreased by thapsigargin (TG). This observation is compatible with other studies that reported a loss of PLB-SERCA crosslinking with TG but appears inconsistent with reported IP experiments. We measured FRET in a heterogeneous population of cells displaying a wide range of protein concentrations. We observed a decrease in the apparent affinity of PLB for SERCA in the presence of TG. Thus, PLB-SERCA binding was decreased by TG in cells expressing a low protein concentration, but the interaction persisted at high protein concentration. The present results may help reconcile contrasting results reported in the literature and enhance our understanding of the regulation of SERCA by PLB.

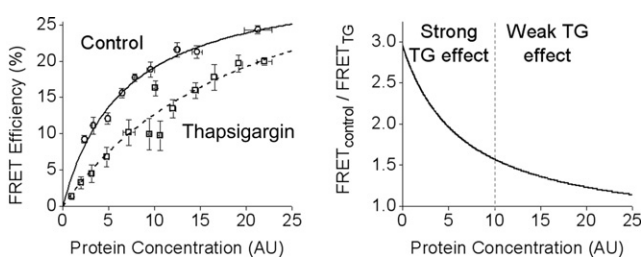

739-Pos Board B618

Collapse of TA-Calmodulin (TACaM) upon Binding to Ca^{2+} Pump Peptide C28 Exposes the TA Moiety to Water and Quenches Its Fluorescence

John T. Penniston[1], Ariel J. Caride[2], Nenad O. Juranic[2], Franklyn G. Prendergast[2], Elena Atanasova[2], Adelaida G. Filoteo[2], Emanuel E. Strehler[2].
[1]Mass. General Hospital, Cambridge, MA, USA, [2]Mayo Clinic, Rochester, MN, USA.

CaM labeled with a fluorescent triazinylaniline (TA) derivative at Lys-75 shows 2 species upon binding to PMCA or to the CaM-binding peptide from PMCA (C28). The 1st, transient, species is slightly more fluorescent than the free CaM, while the 2nd, stable, species is much less fluorescent. The 1st species can also be emulated in a stable form by binding TA-CaM to a shorter peptide, C20. The fluorescence of TA derivatives is quenched and red-shifted by polarizable solvents such as water. $TANMe_2$ has an emission maximum of 391 nm in a non-polar solvent (toluene), which is red-shifted to 419 nm in ethanol (permittivity = 24.5). The emission maxima of TACaM-C20 and TACaM-C28 are 409 nm and 421 nm respectively. Using the Lippert equation, we find that the effective permittivity that TA sees in TACaM-C20 is about 5 and in TACaM-C28 is about 30. Structures of TACaM-C20 (based on 1CFF) and TACaM-C28 (based on our new NMR data on CaM-C28) were made. The C20 complex has the TA residue surrounded by the extended CaM molecule, in an environment containing relatively little water. In the C28 complex the CaM molecule is collapsed. The surroundings of the TA residue are calculated from these molecular structures of hydrated TA-CaM, and the results are comparable with the experimental fluorescence data. (Supported by grants TW06837 and NS51769 from the NIH)

740-Pos Board B619

Distinct Regulation of pH in the Cytosol and in Acidic Organelles by a Subunit Isoforms of V-ATPase in Human Cancer Cells

Souad R. Sennoune[1], Ayana Hinton[2], Sarah Bond[2], Michael Forgac[2], Raul Martinez-Zaguilan[1].
[1]Department of Cell Physiology and Molecular Biophysics, Texas Tech University Health Sciences Center, Lubbock, TX, USA, [2]Department of Physiology, Tufts University School of Medicine, Boston, MA, USA.

V-ATPases are expressed at the plasma membrane (pmV-ATPases) in highly metastatic cells, in addition to their typical distribution in acidic organelles [endosomes/lysosomes (E/L)]. Distinct a subunit isoforms of V-ATPase target the V-ATPase to different cellular membranes. There are 4 a subunit isoforms (a1, a2, a3, and a4). The a3 and a4 isoforms are found at the plasma membrane in osteoclasts and renal intercalated cells, respectively. We employed isoform-specific siRNA to selectively reduced the mRNA levels of each isoform in highly metastatic human melanoma (C8161) and breast (MB231) cancer cells. Inhibition of V-ATPase with concanamycin decreased in vitro cell invasion. Knockdown of either a3 or a4 also inhibits cell invasion. Simultaneous measurements of pH in the cytosol (pH^{cyt}) and in E/L ($pH^{E/L}$) using pH fluoroprobes targeted to the cytosol or E/L indicated that in C8161 cells, the steady state pH^{cyt} was more acidic in cells transduced with either siRNA-a3 or -a4. Knockdown of a3 in MB231 decreased pH^{cyt}, whereas siRNA-a1, -a2 and -a4 did not affect pH^{cyt}. The $pH^{E/L}$ was more alkaline by knockdown of either a1, a2, or a3 in MB231, whereas in C8161 the $pH^{E/L}$ was increased by siRNA-a1 or -a2. The proton fluxes following an acid load were significantly decreased by knockdown of a1, a2, and a3 in MB231 cells. These data suggest that specific a subunits of V-ATPase control pH in E/L and the cytosol in highly metastatic cells; and that a3 and a4 are significant for pH regulation across the plasma membrane, whereas a1, a2 and a3 are important for $pH^{E/L}$ regulation. These data emphasize the significance of a3 and a4 for the acquisition of an invasive phenotype in metastatic cells.

741-Pos Board B620

Direct Observation Of Rotation Of F1-Atpase From Saccharomyces cerevisiae With mgi Mutations

Bradley C. Steel[1], Yamin Wang[2], Vijay Pagadala[2], Richard M. Berry[1], David M. Mueller[2].
[1]University of Oxford, Oxford, United Kingdom, [2]Rosalind Franklin University of Medicine and Science, Chicago, IL, USA.

Mitochondrial Genome Instability (*mgi*) mutations allow yeast to survive the loss of mitochondrial DNA. A number of these mutations occur in the genes encoding the F_1 portion of the ATP Synthase, and have been shown to uncouple ATP Synthase (Wang et al. 2007). The mutations cluster around the collar region of F_1 where the alpha, beta and gamma subunits interact and are thus likely to affect the kinetics of F_1 rotation.

Single molecule studies of the thermophilic *Bacillus* PS3 F_1-ATPase have revealed kinetic and structural information that cannot be discerned using other